Cardiovascular Diabetology

RESEARCH

Open Access

Interdependence between myocardial deformation and perfusion in patients with T2DM and HFpEF: a feature-tracking and stress perfusion CMR study

Xin-Ni Li[1], Yu-Ting Liu[1], Sang Kang[1], Dan Zeng Qu Yang[1], Huo-Yuan Xiao[1], Wen-Kun Ma[1], Cheng-Xing Shen[1*] and Jing-Wei Pan[1*]

Abstract

Background Patients with diabetes have an increased risk of developing heart failure with preserved ejection fraction (HFpEF). This study aimed to compare indices of myocardial deformation and perfusion between patients with type 2 diabetes mellitus (T2DM) with and without HFpEF and to investigate the relationship between myocardial strain and perfusion reserve.

Methods This study included 156 patients with T2DM without obstructive coronary artery disease (CAD) and 50 healthy volunteers who underwent cardiac magnetic resonance (CMR) examination at our center. Patients with T2DM were subdivided into the T2DM–HFpEF (n = 74) and the T2DM–non-HFpEF (n = 82) groups. The parameters of left ventricular (LV) and left atrial (LA) strain as well as stress myocardial perfusion were compared. The correlation between myocardial deformation and perfusion parameters was also assessed. Mediation analyses were used to evaluate the direct and indirect effects of T2DM on LA strain.

Results Patients with T2DM and HFpEF had reduced LV radial peak systolic strain rate (PSSR), LV circumferential peak diastolic strain rate (PDSR), LA reservoir strain, global myocardial perfusion reserve index (MPRI), and increased LA booster strain compared to patients with T2DM without HFpEF (all $P < 0.05$). Furthermore, LV longitudinal PSSR, LA reservoir, and LA conduit strain were notably impaired in patients with T2DM without HFpEF compared to controls (all $P < 0.05$), but LV torsion, LV radial PSSR, and LA booster strain compensated for these alterations (all $P < 0.05$). Multivariate linear regression analysis demonstrated that LA reservoir and LA booster strain were independently associated with global MPRI ($\beta = 0.259$, $P < 0.001$; $\beta = -0.326$, $P < 0.001$, respectively). Further, the difference in LA reservoir and LA booster strain between patients with T2DM with and without HFpEF was totally mediated by global MPRI. Global stress PI, LA booster, global rest PI, and global MPRI showed high accuracy in diagnosing HFpEF among patients with T2DM (areas under the curve [AUC]: 0.803, 0.790, 0.740, 0.740, respectively).

*Correspondence:
Cheng-Xing Shen
shencx@sjtu.edu.cn
Jing-Wei Pan
jwpan@sjtu.edu.cn

Full list of author information is available at the end of the article

Conclusions Patients with T2DM and HFpEF exhibited significant LV systolic and diastolic deformation, decreased LA reservoir strain, severe impairment of myocardial perfusion, and elevated LA booster strain that is a compensatory response in HFpEF. Global MPRI was identified as an independent influencing factor on LA reservoir and LA booster strain. The difference in LA reservoir and LA booster strain between patients with T2DM with and without HFpEF was totally mediated by global MPRI, suggesting a possible mechanistic link between microcirculation impairment and cardiac dysfunction in diabetes. Myocardial perfusion and LA strain may prove valuable for diagnosing and managing HFpEF in the future.

Keywords Diabetes mellitus, Heart failure, Myocardial dysfunction, Myocardial perfusion, CMR feature-tracking

Background

Diabetes mellitus (DM) is a group of metabolic disorders that leads to the underutilization and overproduction of glucose [1]. Many symptomatic patients with verified cardiac ischemia do not have obstructive coronary artery disease (CAD), and this can be explained by a diffuse pathology appearing as mild or moderate lesions on coronary angiography, dynamic stenoses of epicardial vessels, or coronary microvascular dysfunction (CMD) [2, 3]. CMD can be diagnosed in the majority of patients with diabetes and angina who have no significant coronary lesions [4]. Furthermore, patients with diabetes have an increased risk of developing cardiovascular disease (CVD) and heart failure (HF) [5]. Rates of HF hospitalization are twice as high in people with diabetes compared to those without this condition [6, 7].

Myocardial deformation, comprising both global and regional myocardial function, has emerged as a potential marker of subtle changes in left ventricular (LV) function and is being increasingly viewed as a more sensitive indicator of cardiac insufficiency [8–11]. Studies have suggested that LV diastolic dysfunction appears early and is the most prominent characteristic of diabetic heart disease, along with myocardial remodeling [12, 13]. Apart from LV dysfunction, multiple studies have confirmed that left atrial (LA) maximum volume strongly correlates with cardiovascular outcomes and this improves the assessment of LV diastolic function [14, 15]. Recent studies have demonstrated that LA strain impairment exists in heart failure preserved ejection fraction (HFpEF) and may be one of the initial signs of diastolic dysfunction [16–19]. Previous studies on LA strain mainly focused on patients with dilated cardiomyopathy, hypertensive cardiomyopathy (HCM), and dialysis [20–22], with few studies on patients with type 2 diabetes mellitus (T2DM), especially those with HFpEF. Furthermore, previous studies have demonstrated that patients with T2DM have impaired myocardial perfusion, as represented by a reduced myocardial perfusion reserve index (MPRI), a semi-quantifiable parameter associated with LV diastolic dysfunction [23, 24]. However, the association between myocardial perfusion and myocardial deformation remains largely unexplored, and no studies have investigated the interdependence of myocardial deformation and perfusion in patients with T2DM and HFpEF.

Cardiac magnetic resonance (CMR) feature tracking is a promising technique that allows the evaluation of longitudinal, circumferential, and radial myocardial deformation with high sensitivity and reproducibility [25, 26]. Additionally, stress perfusion CMR allows noninvasive monitoring of myocardial microvascular dysfunction.

In this study, we aimed to (1) compare indices of myocardial deformation and perfusion between patients with T2DM with and without HFpEF; (2) investigate the relationship between myocardial strain and perfusion parameters; and (3) assess the mediating effects of impaired myocardial perfusion on LA strain in patients with T2DM.

Methods

Study population

The study was approved by the Ethics Committee of our institution (Ethics Approval Number: 2021–250). Informed consent was obtained from all the participants. A total of 175 patients with T2DM who experienced shortness of breath or atypical chest tightness symptoms between June 2021 and June 2023 were prospectively included. Patients with obstructive CAD (stenosis ≥ 50%) were excluded based on coronary artery angiography or coronary computed tomographic angiography before undergoing CMR examinations. The diagnostic and classification criteria for T2DM followed the American Diabetes Association standards outlined in the 2024 Standards of Care in Diabetes [1]. HFpEF was defined according to the 2021 European Society of Cardiology (ESC) Guidelines for the diagnosis and treatment of acute and chronic heart failure as follows: (1) Symptoms and signs of HF; (2) Left ventricular ejection fraction (LVEF) ≥ 50%.; (3) Objective evidence of cardiac structural and/or functional abnormalities consistent with the presence of LV diastolic dysfunction or elevated LV filling pressures, including increased levels of natriuretic peptides (NPs) [27]. Exclusion criteria included previous myocardial infarction, previous coronary artery bypass surgery, cardiomyopathy, bundle branch block, atrial fibrillation, moderate to severe valvular heart disease confirmed by echocardiography, severe renal failure

(estimated glomerular filtration rate [eGFR] < 30 mL/min/1.73 m^2), contraindications to CMR or adenosine, inadequate hemodynamic response, confirmed claustrophobia or poor image quality [28]. For comparison, we recruited 55 age- and sex-matched volunteers with no history of T2DM or cardiac disease who underwent identical CMR examinations.

Baselines data collection

Demographic characteristics and clinical information were recorded from the electronic medical records system of our hospital. Blood samples for standard laboratory analyses were obtained from participants and processed using the central clinical laboratory protocols of our hospital.

Echocardiography

All participants underwent two-dimensional, M-mode and tissue Doppler echocardiography by an experienced cardiologist using a Vivid E9 equipped with an M5S 3.5–5 MHz transducer (GE Vingmed Ultrasound, Horten, Norway) from three consecutive cardiac cycles in the left lateral decubitus position. The current analysis focused on the following LV and LA structural parameters: relative wall thickness (RWT), left ventricular mass index (LVMI), and left atrial volume index (LAVI). RWT was defined as the ratio of (2×LV posterior wall thickness at end-diastolic dimension) / LV end-diastolic dimension. LVMI was calculated by dividing left ventricular mass by the body surface area (BSA). LAVI was calculated by dividing the left atrial volume by the BSA. LVEF was calculated from the apical four and two-chamber views using the biplane Simpson's method. The LV diastolic function was measured through the apical four-chamber view. Peak velocity in early diastole of mitral valve inflow (E) was measured by placing a pulse wave Doppler across the mitral valve and early diastolic velocity of the mitral valve annulus (e′) was measured by using tissue Doppler imaging and by placing a pulse wave Doppler in the lateral and septal mitral annulus. The mean E/e′ ratio was then calculated.

CMR protocol

CMR examinations were performed with patients in the supine position using a 3.0 Tesla whole-body scanner (MAGNETOM Trio Tim; Siemens Healthcare, Erlangen, Germany) equipped with an 18-channel body coil and a 32-channel spine coil. A standard electrocardiographic (ECG) triggering device was used synchronously and data were acquired at the end-expiratory breath-hold. A balanced steady-state free precession (bSSFP) sequence (repetition time [TR]/echo time [TE], 45.08/1.22 ms; flip angle, 49°; slice thickness, 8 mm; field of view, 360×300 mm^2; matrix size, 256×216; and temporal resolution, 39.34 ms) was used to acquire 8 to 12 continuous cine images of the LV short-axis view (from the basal to the apex), as well as the long-axis view of LV (two-, three- and four-chamber views).

Briefly, stress perfusion was conducted during maximal vasodilation, stimulated by intravenous adenosine infusion at a dose of 140 μg/kg/min for 4 min. An adequate hemodynamic response was indicated by a heart rate increase of ≥ 10% and or systolic blood pressure drop of ≥ 10 mmHg [28]. For perfusion imaging, a dose of 0.2 mL/kg gadobenate dimeglumine (MultiHance 0.5 mmol/mL; Bracco, Milan, Italy) was injected automatically using an automated injector (Optistar Elite, Mallinckrodt, Cincinnati, OH, USA) at a flow rate of 3.0–3.5 mL/s, followed by 20 mL saline at a flow rate of 3.0 mL/s. The images were captured simultaneously using intravenous contrast agents and an inversion recovery echo-planar imaging (IR-EPI) sequence (TR/TE, 95.6/1.03 ms; flip angle, 10°; slice thickness, 8 mm; field of view, 360×270 mm^2; and matrix size, 256×192). Three standard short-axis slices of the LV (basal, middle, and apical) and one four-chamber view slice were used for imaging. The first-past rest perfusion scan was conducted in identical slice locations after a 10-min delay to wash out the adenosine, following the same approach as for the stress perfusion scan. Late gadolinium enhancement (LGE) imaging was also performed using a segmented-turbo-FLASH phase-sensitive inversion recovery (PSIR) sequence (TR/TE, 765.0/1.96 ms; flip angle, 20°; slice thickness, 8 mm; field of view, 360×270 mm^2; and matrix size, 256×192) 10–15 min after the second contrast administration.

CMR image analysis

CMR images were analyzed using commercial software (cvi42, version 5.10.1, Circle Cardiovascular Imaging, Calgary, AB, Canada) by two observers (SK and YTL) who were blind to the clinical details of the participants. Cardiac function parameters were calculated by manually tracing the endocardial and epicardial contours in serial short-axis cine images at end-diastole and end-systole, respectively. The 3-dimensional tissue tracking module was used to analyze the LV myocardial strain by loading long-axis two-chamber, four-chamber, and short-axis slices. Finally, LV torsion, the biventricular global radial, circumferential, and longitudinal peak systolic strain rate (PSSR), and peak diastolic strain rate (PDSR) were automatically computed through feature-tracking analysis. The LA strain is characterized by three phases: reservoir function, conduit function, and booster function [19]. LA endocardial and epicardial border contours were initially traced in apical four-chamber and two-chamber views at the end-diastole, with LA strain values automatically derived and averaged using the software (Fig. 1). To

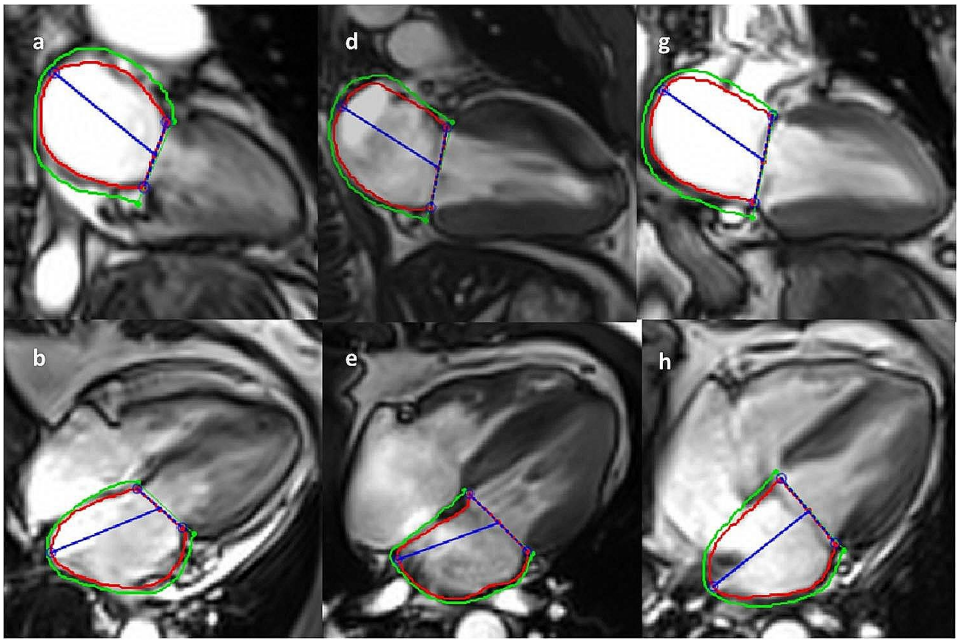

Fig. 1 Representative example of left atrial (LA) tracking analysis by cvi42 software (Circle Cardiovascular Imaging, Calgary, AB, Canada) in the four- and two-chamber views at end-diastole among the control group, the T2DM–non-HFpEF group, and the T2DM–HFpEF group (**a**–**b**, **d**–**e**, and **g**–**h**)

evaluate myocardial perfusion, the endocardial and epicardial contours were manually delineated, along with a region of interest (ROI) drawn from the LV blood pool. Careful selection of the ROI was made to exclude the adjacent blood pool and epicardium to allow for the formation of an arterial input function. Furthermore, myocardial perfusion upslopes (perfusion index [PI]) during rest and stress were calculated using a 5-point linear-fit model of SI versus time and normalized to the LV blood pool upslope. The MPRI is defined as the ratio of stress to rest upslope normalized to the upslope of the blood pool and represents the vasodilation capacity of small vessels [29]. The LV myocardium was divided into 16 segments according to the recommendations of the American Heart Association, and perfusion parameters were automatically computed via cvi42 software. The global MPRI was calculated as the mean value of 16 segments. Inter-rater agreement was assessed through the analysis of 10 randomly selected participants by two independent CMR analysts (SK and YTL), and intra-observer variability was evaluated by re-analysis of 10 participants after 1 month. The intraclass correlation coefficient (ICC) was used to evaluate inter- and intra-observer variabilities.

Statistical analysis

Statistical analyses were performed using SPSS software version 25.0.0.1 (IBM Corporation, located in Armonk, NY, USA), and Prism software version 8.4.0 (GraphPad Software, Inc., located in San Diego, CA, USA). All data were checked for normality using the Kolmogorov–Smirnov test and presented as mean ± standard deviation (SD). Non-normally distributed data were expressed as medians, while categorical data were presented as numbers and percentages. The chi-squared test was used to compare categorical data. Independent sample t-tests were applied for normally distributed data and the Mann–Whitney U test for non-normally distributed data in two-group comparisons, whereas one-way analysis of variance was used for multiple-group comparisons. Kruskal–Wallis rank tests were used to analyze parameters that did not conform to normality or exhibited homogeneity in variance. ICC was used to evaluate inter- and intra-observer variabilities. Pearson's correlation coefficient was employed in the study to determine the relationship between LV and LA myocardial strain parameters, as well as myocardial strain and perfusion indicators. Univariate linear regression analysis was considered significant at $P<0.05$. These variables, without collinearity, were then included in the backward stepwise multivariate analysis that aimed to identify the independent determinants of LA reservoir strain and booster strain. All analyses were performed using a two-sided significance level of $P<0.05$. Mediation analyses were carried out using the bootstrap method to assess whether

LV strain and myocardial perfusion mediated the changes in LA reservoir strain and booster strain in a statistically significant manner among patients with T2DM with and without HFpEF. The LV circumferential PDSR and global MPRI that are affected by diabetes, were included as mediators in the aforementioned regression models. The area under the receiver operating characteristic (ROC) curve (AUC), sensitivity, specificity, positive predictive value (PPV), and negative predictive value (NPV) was calculated to evaluate the diagnostic ability of the CMR parameters to distinguish HFpEF. The optimal cut-off values were determined using the Youden index.

Results

Baseline characteristics

A total of 175 patients with T2DM and 55 age- and sex-matched healthy controls were enrolled in this study. However, 11 patients with T2DM exhibited≥1 exclusion criteria, while participants with myocardial infarction (T2DM group [n=3]) or poor image quality (T2DM group [n=5], and control group [n=5]) were also excluded. Finally, 156 patients with T2DM and 50 healthy controls were included in this study. The T2DM cohort was further divided into two groups: T2DM–HFpEF (n=74) and T2DM–non-HFpEF groups (n=82) (Fig. 2). T2DM–HFpEF group tended to be associated with higher Fibrosis-4 index (Fib-4), glycosylated hemoglobin (HbA1c) levels, B-type natriuretic peptide (BNP) levels, pro-B-type natriuretic peptide (pro-BNP) levels,

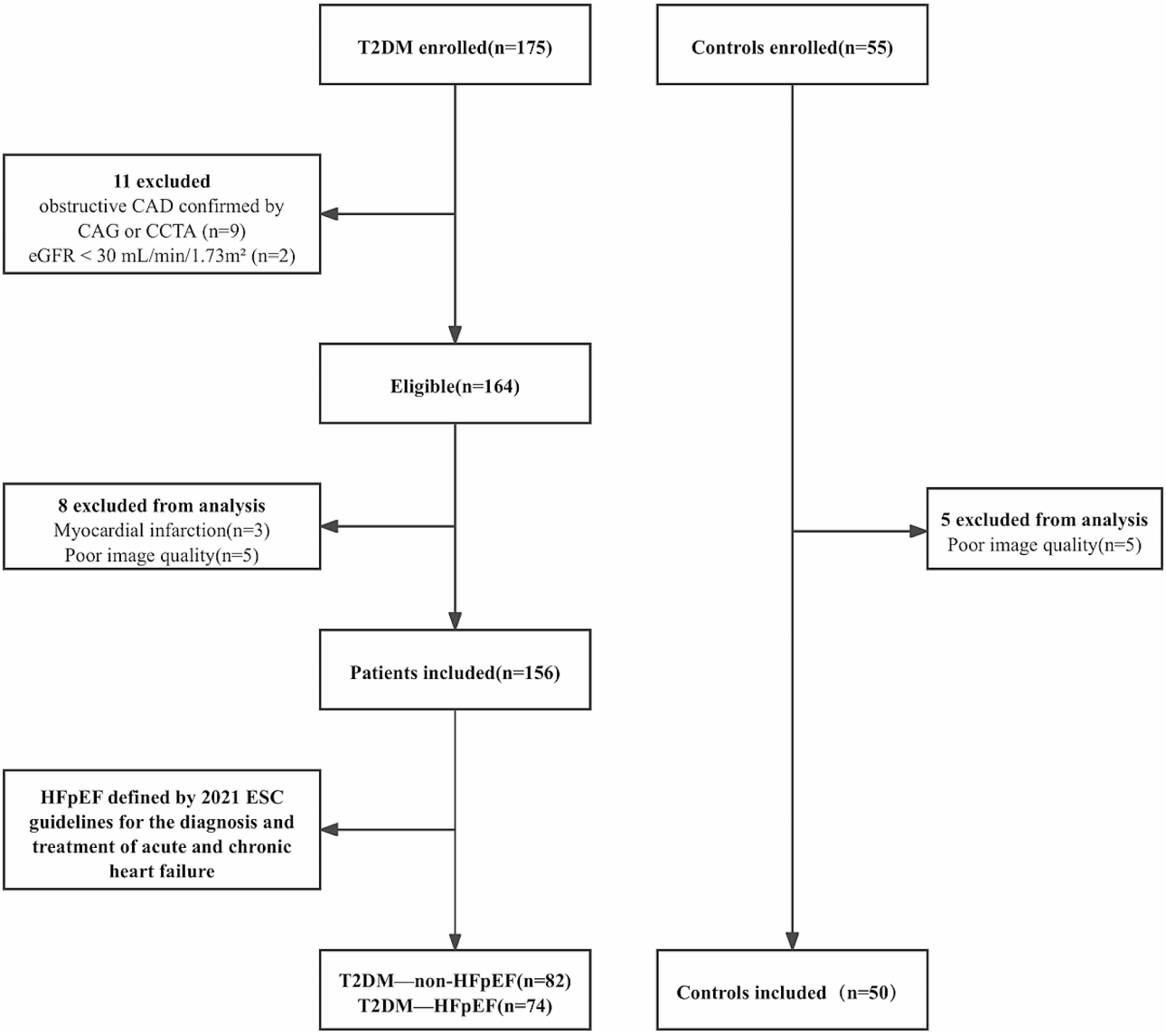

Fig. 2 Flow diagram of study recruitment

uric acid (UA) levels, and total cholesterol (TC) levels, increased mean E/e′ and LAVI, and longer hypertension duration and diabetes duration (all $P<0.05$). A borderline significance existed in body mass index (BMI) among the three groups. ($P=0.058$). There were no significant differences in age, sex, BSA, and serum creatinine (Scr) levels between the three groups (all $P>0.05$) (Table 1).

Comparison of CMR findings among groups

The results of CMR imaging for global LV and LA strain are shown in Table 2. Within the two T2DM patient groups, LV radial PSSR, LV circumferential PDSR, and LA reservoir strain were significantly reduced in patients with T2DM with HFpEF than in patients with T2DM without HFpEF (all $P<0.001$), while LA booster strain increased significantly (all $P<0.001$) (Fig. 3). Furthermore, the LV longitudinal PSSR, LA reservoir, and LA conduit strain were notably impaired in patients with T2DM without HFpEF compared with controls (all $P<0.05$); however, LV torsion, LV radial PSSR, and L A booster strain compensated for these alterations (all $P<0.05$). Additionally, LV torsion and LA booster strain were significantly greater (all $P<0.001$), while LV longitudinal PSSR, LV circumferential PSSR, LA reservoir, and LA conduit strain were considerably lower in the T2DM–HFpEF group compared to the control group (all $P<0.001$) (Fig. 3).

Data on global first-pass perfusion parameters are also summarized in Table 2. There were significant differences in global rest PI, global stress PI, and global MPRI among the three groups (all $P<0.001$). Within the two T2DM patient groups, the global rest PI, global stress PI, and global MPRI were also significantly decreased in patients with T2DM and HFpEF (all $P<0.05$) (Fig. 3).

Association between myocardial strain and perfusion

LV longitudinal PDSR was significantly associated with LA reservoir strain (r=0.149, $P<0.033$). LV longitudinal

Table 1 Baseline characteristics of the study cohort

	Control n = 50	T2DM–non-HFpEF n = 82	T2DM–HFpEF n = 74	*P*-value
Demographics				
Age, years	59.70 ± 9.73	58.05 ± 9.42	61.00 ± 9.73	0.160
Male, n (%)	22 (44.0%)	42 (41.2%)	36 (35.3%)	0.922
BMI, kg/m^2	26.17 (23.05,27.68)	24.22 (22.36,26.41)	24.97 (21.82,26.71)	0.058
BSA, m^2	1.79 ± 0.18	1.80 ± 0.17	1.75 ± 0.20	0.320
HR, bpm	65.04 ± 10.68	76.09 ± 10.12*	75.19 ± 13.52*	< 0.001$^\#$
TyG-BMI	9.20 (8.92,11.69)	14.95 (12.38,15.74)*	15.88 (12.56,17.43)*	< 0.001$^\#$
Fib-4	0.55 (0.53,0.76)	0.72 (0.66,1.00)*	1.30 (1.00,1.46)$^{*\&}$	< 0.001$^\#$
Laboratory test				
FBG, mmol/L	5.22 ± 0.19	6.88 ± 1.28*	7.03 ± 1.84*	< 0.001$^\#$
HbA1c, %	5.73 ± 0.20	6.65 ± 0.70*	7.18 ± 0.93$^{*\&}$	< 0.001$^\#$
BNP, pg/mL	22.00 (16.38,30.50)	35.00 (27.88,43.50)*	139.00 (77.50,191.50)$^{*\&}$	< 0.001$^\#$
proBNP, ng/L	65.25 (48.38,123.50)	155.00 (135.00,211.00)*	372.00 (290.50,492.00)$^{*\&}$	0.007$^\#$
Scr, μmol/L	67.66 ± 8.43	71.48 ± 14.46	67.96 ± 12.90	0.132
UA, μmol/L	325.77 ± 73.36	402.32 ± 53.81*	232.62 ± 110.61$^{*\&}$	< 0.001$^\#$
TC, mmol/L	3.18 (3.17,4.72)	3.44 (3.40,3.93)*	4.03(3.53,4.73)$^{*\&}$	< 0.001$^\#$
TG, mmol/L	0.96 (0.93,1.23)	1.47 (0.96,1.84)*	1.30 (0.96,2.89)*	< 0.001$^\#$
HDL, mmol/L	1.47 (1.37,1.56)	1.25 (1.09,1.32)*	1.23 (1.07,1.40)*	< 0.001$^\#$
LDL, mmol/L	1.83 ± 0.65	2.39 ± 0.63*	2.21 ± 0.50*	< 0.001$^\#$
Echocardiography				
LVEF, %	62.54 ± 2.13	63.50 ± 1.44*	61.38 ± 2.62$^{*\&}$	< 0.001$^\#$
RWT, ratio	0.30 ± 0.03	0.35 ± 0.04*	0.36 ± 0.05*	< 0.001$^\#$
Mean E/e′, ratio	8.78 ± 0.90	8.50 ± 0.93	11.63 ± 2.54$^{*\&}$	< 0.001$^\#$
LVMI, g/m^2	58.50 (48.61,59.95)	50.18 (44.43,50.22)	44.85 (42.68,54.19)*	0.004$^\#$
LAVI, mL/m^2	15.64 (14.2,15.90)	16.32 (10.90,18.39)	17.14 (14.32,26.89)$^{*\&}$	0.002$^\#$
Medical history				
Hypertension duration, years	0.17(0.04,0.50)	8.00 (0.00,12.00)*	10.00 (2.00,20.00)$^{*\&}$	< 0.001$^\#$
Diabetes duration, years	–	9.24 ± 4.20*	12.23 ± 7.79$^{*\&}$	< 0.001$^\#$

Data are presented as the mean ± SD, n (%) or median (IQR). Dash (–) indicates not applicable

HFpEF Heart failure with preserved ejection fraction, *BMI* body mass index, *BSA* body surface area, *HR* heart rate, *TyG-BMI* triglyceride glucose-body mass index, *Fib-4* Fibrosis-4 index, *FBG* fasting blood glucose, *HbA1c* glycosylated hemoglobin, *BNP* B-type natriuretic peptide, *proBNP*, pro-B-type natriuretic peptide, *Scr* serum creatinine, *UA* uric acid, *TC* total cholesterol, *TG* total triglyceride, *HDL* high-density lipoprotein, *LDL* low-density lipoprotein, *RWT* relative wall thickness, E/e' early filling velocity on transmitral Doppler/early relaxation velocity on tissue Doppler, *LVMI* left ventricular mass index, *LAVI* left atrial volume index

$^*p<0.05$ vs. control group; $^\&p<0.05$ vs. T2DM–non-HFpEF; $^\#p<0.05$

Table 2 CMR findings in 3 groups

	Control n = 50	T2DM–non-HFpEF n = 82	T2DM–HFpEF n = 74	*P*-value
CMR–LV strain				
Torsion, °/cm	1.36 (1.32, 1.73)	1.52 (1.48, 1.97)*	1.54 (1.52, 1.62)*	< 0.001#
PSSR, s^{-1}				
Longitudinal	-1.05 ± 0.23	-1.03 ± 0.12	-0.98 ± 0.22	0.089
Circumferential	-1.00 ± 0.05	-1.00 ± 0.08	-1.00 ± 0.14	0.995
Radial	1.81 ± 0.07	1.87 ± 0.19*	1.79 ± 0.11&	< 0.001#
PDSR, s^{-1}				
Longitudinal	1.34 ± 0.32	1.04 ± 0.11*	1.04 ± 0.21*	< 0.001#
Circumferential	1.13 ± 0.27	1.06 ± 0.46	0.73 ± 0.52*&	< 0.001#
Radial	-2.12 ± 1.13	-2.18 ± 1.19	-2.12 ± 0.70	0.937
CMR–LA strain				
Reservoir, %	44.88 ± 2.57	43.45 ± 3.68*	41.93 ± 2.75*&	< 0.001#
Conduit, %	31.39 ± 2.53	28.98 ± 1.60*	28.69 ± 3.22*	< 0.001#
Booster, %	14.65 ± 1.24	16.34 ± 1.48*	17.99 ± 1.74*&	< 0.001#
CMR–perfusion				
Global rest PI	0.14 ± 0.05	0.12 ± 0.02*	0.11 ± 0.03*&	< 0.001#
Global stress PI	0.24 ± 0.08	0.16 ± 0.02*	0.13 ± 0.02*&	< 0.001#
Global MPRI, ratio	1.71 ± 0.26	1.28 ± 0.10*	1.20 ± 0.11*&	< 0.001#

Values are presented as the mean ± SD or median (IQR)

HFpEF Heart failure with preserved ejection fraction, *LVEF* left ventricular ejection fraction, *PI* perfusion index, *MPRI* myocardial perfusion reserve index, *PSSR* peak systolic strain rate, *PDSR* peak diastolic strain rate

*$p < 0.05$ vs. control group; &$p < 0.05$ vs. T2DM–non-HFpEF group; #$p < 0.001$

PSSR, LV longitudinal PDSR, and LV circumferential PDSR were positively associated with LA conduit strain (r = 0.161, $P = 0.021$; r = 0.204, $P = 0.003$; and r = 0.141, $P = 0.043$, respectively), whereas LV longitudinal PDSR was negatively associated with LA booster strain (r = − 0.254, $P < 0.001$) (Supplementary Table 1). In addition, LV longitudinal PDSR, LV circumferential PDSR, LA reservoir, and LA conduit strain were associated with global MPRI (r = 0.451, $P < 0.001$; r = 0.156, $P = 0.025$; r = 0.259, $P < 0.001$; and r = 0.294, $P < 0.001$, respectively). Further, global MPRI was inversely correlated with LA booster strain (r = − 0.455, $P < 0.001$) (Supplementary Table 2).

Multivariate linear regression analysis demonstrated that LA reservoir strain was independently associated with global MPRI (β = 0.259, $P < 0.001$) (Table 3). In addition, LA booster strain was independently associated with global rest PI, global MPRI, and HbA1c levels (β = − 0.126, $P = 0.045$; β = − 0.326, $P < 0.001$; and β = 0.204, $P = 0.004$, respectively) (Table 4)

Direct and indirect effects of DM on LA strains

The direct and indirect effects of T2DM on LA strain with mediators of LV circumferential PDSR and global MPRI are shown in Table 5. The difference in LA reservoir strain between the T2DM–non-HFpEF group and the T2DM–HFpEF group was totally mediated by global MPRI (indirect effecting: 0.276, bootstrapped 95%CI 0.105–0.528), and LV circumferential PDSR had no significant mediating effect. The difference in LA booster strain between the T2DM–non-HFpEF group and the T2DM–HFpEF group was totally mediated by global MPRI (indirect effecting: − 0.290, bootstrapped 95%CI − 0.523–− 0.121), while LV circumferential PDSR had no significant mediating effect.

Diagnostic ability of the CMR parameters in HFpEF

Table 6 displays the diagnostic performance of myocardial deformation and perfusion indices. AUC was highest for LA booster (0.857), followed by global stress PI (0.848) and global MPRI (0.808) (Fig. 4). Global stress PI, LA booster, global rest PI, and global MPRI exhibited the highest AUC (0.803, 0.790, 0.740, 0.740, respectively), all of which far exceeded the predictive ability of LAVI (0.690), distinguished T2DM patients with and without HFpEF (Fig. 4).

Intra-observer and inter-observer variability

Excellent intra- and inter-observer agreement was observed in the measurement of myocardial strain (ICC = 0.748–0.992 and 0.766–0.980, respectively) and myocardial perfusion (ICC = 0. 748–0.961 and 0.921–0.942, respectively) (Supplementary Table 3).

Discussions

This study aimed to investigate the impairment of cardiac function and myocardial perfusion reserve in patients with T2DM and to highlight the complicated interplay between myocardial strain and perfusion, particularly in the HFpEF population. First, compared to controls, patients with T2DM exhibited both systolic and diastolic dysfunction, reduced LA reservoir and LA conduit strain, and impaired myocardial perfusion but increased LV torsion and LA booster strain. This suggests that patients with T2DM exhibit compromised myocardial strain and perfusion; however, there is a compensatory increase in LV torsion and LA contraction. Second, patients with T2DM and HFpEF displayed a more severe systolic and diastolic dysfunction, reduced LA reservoir strain, impaired myocardial perfusion, and elevated LA booster strain than patients with T2DM without HFpEF. Third, global MPRI was identified as an independent factor influencing LA reservoir strain, as were global rest PI, global MPRI, and HbA1c levels for LA booster strain. Further, the observed differences in LA reservoir and LA booster strain between patients with T2DM without HFpEF and those with HFpEF were solely mediated by global MPRI.

LV torsion has been recognized as a critical mechanism for maintaining normal cardiac function [30]. It has

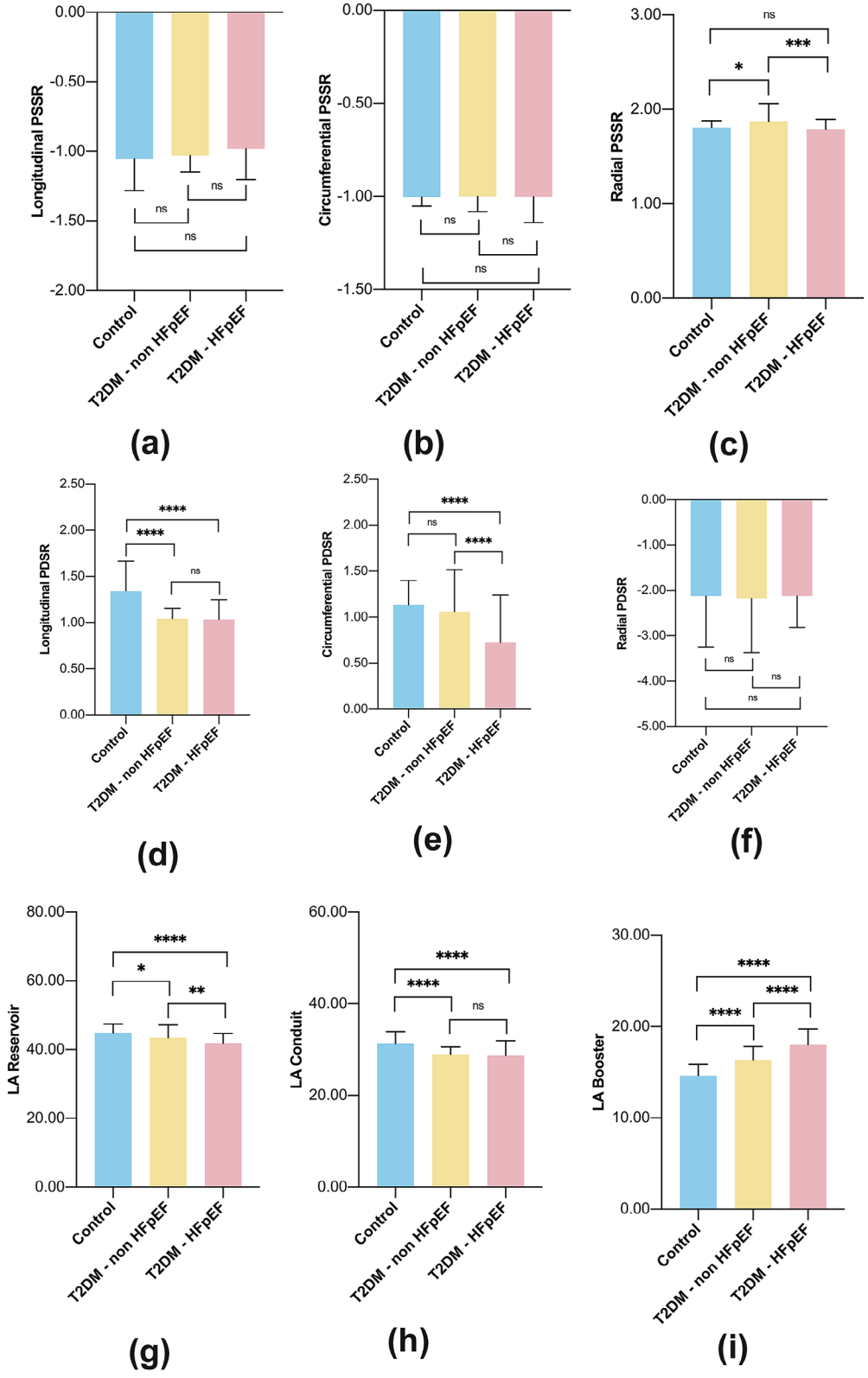

Fig. 3 Difference in LV strain, LA strain, and myocardial perfusion among the control group, the T2DM–non-HFpEF group and the T2DM-HFpEF group. LV longitudinal peak systolic strain rate (PSSR) (**a**), LV circumferential PSSR (**b**), LV radial PSSR (**c**), LV longitudinal peak diastolic strain rate (PDSR) (**d**), LV circumferential PDSR (**e**), LV radial PDSR (**f**), Left atrial (LA) reservoir strain (**g**), LA conduit strain (**h**), LA booster strain (**i**), global rest perfusion index (PI) (**j**), global stress PI (**k**) and global myocardial perfusion reserve index (MPRI) (**l**) among the three groups. ns: $P > 0.05$; *$P < 0.05$; **$P < 0.01$; ***$P < 0.001$; ****$P < 0.0001$

Table 3 Associations between LA reservoir strain and LV longitudinal PDSR, rest PI, and global MPRI in the whole participants

	LA reservoir strain			
	Univariate		Multivariate	
	β	*P*	β	*P*
LV longitudinal PDSR, s^{-1}	0.149	0.033	-	-
global stress PI	0.183	0.008	-	-
global MPRI, ratio	0.259	< 0.001	0.259	< 0.001
HbA1c, %	-0.135	0.054	-	-

β is adjusted regression coefficient. Factors with $P<0.1$ in the univariable analyses were included in the backwards stepwise multiple linear regression model

Left atrial (LA), left ventricular (LV), longitudinal peak diastolic strain rate (PDSR), perfusion index (PI), myocardial perfusion reserve index (MPRI), glycosylated hemoglobin (HbA1c)

Table 4 Associations between LA booster strain and LV longitudinal PDSR, LV circumferential PDSR, global rest PI, global stress PI, and global MPRI in the whole participants

	LA booster strain			
	Univariate		Multivariate	
	β	*P*	β	*P*
LV longitudinal PDSR, s^{-1}	-0.254	< 0.001	-	-
LV circumferential PDSR, s^{-1}	-0.137	0.049	-	-
global rest PI	-0.240	0.001	-0.126	0.045
global stress PI	-0.374	< 0.001	-	-
global MPRI, ratio	-0.455	< 0.001	-0.326	< 0.001
HbA1c, %	0.398	< 0.001	0.204	0.004

β is adjusted regression coefficient. Factors with $P<0.1$ in the univariable analyses were included in the backwards stepwise multiple linear regression model

LA Left atrial, *LV* left ventricular, *PDSR* peak diastolic strain rate, *PI* perfusion index, *MPRI* myocardial perfusion reserve index, *HbA1c* glycosylated hemoglobin

Table 5 Mediating effects of T2DM on LA reservoir strain and LA booster strain with mediators of LV circumferential PDSR and global MPRI

	LA reservoir strain		LA booster strain	
	Direct effect	Indirect effect	Direct effect	Indirect effect
LV circumferential PDSR, s^{-1}	0.236 (-0.710, 1.182)	0.067 (-0.210, 0.356)	-0.286 (-0.808, 0.236)	-0.082 (-0.249, 0.046)
global MPRI, ratio	3.248(1.515, 4.981)*	0.276 (0.105, 0.528)*	-3.412 (-4.368, -2.456)*	-0.290 (-0.523, -0.121)*

LA left atrial, *LV* left ventricular, *PDSR* peak diastolic strain rate, *MPRI* myocardial perfusion reserve index

been hypothesized that enhanced LV torsion may act as a compensatory mechanism for the pathologically reduced longitudinal function [31]. Increased LV torsion has been found to be related to glycemic states across the clinical spectrum, from non-DM to DM, and is in line with the impaired longitudinal function that has been reported in studies [32, 33]. The potential mechanism of enhanced LV torsion in patients with T2DM remains incompletely understood and is possibly related to changes in the extracellular matrix that impact the storing potential energy during the twisting motion of the spiraling myofibers of the LV [34]. Besides, LV torsion is caused by the dynamic interaction between oppositely oriented subepicardial and subendocardial myocardial fibre helices. The direction of LV twist is governed by the subepicardial fibres, mainly owing to their longer arm of movement. Therefore, another possible explanation of enhanced LV torsion in patients with T2DM is the diminished counteraction of the subendocardial myofibres caused by subendocardial ischemia or dysfunction [35, 36].

The prevalence of HF has increased to 22% in patients with T2DM [37]. Individuals with T2DM have reduced global LV longitudinal, circumferential, and radial PDSR compared to healthy individuals [38]. Another study revealed that patients with T2DM had higher LV longitudinal and radial PSSR and lower LV longitudinal, circumferential, and radial PDSR than healthy controls [39]. The results of our study on LV myocardial deformation in patients with T2DM are consistent with those of other studies. We explored these parameters in patients with T2DM and HFpEF and found that LV radial PSSR and LV circumferential PDSR were significantly decreased in patients with T2DM and HFpEF compared to patients with T2DM without HFpEF, suggesting that significant alterations in cardiac mechanics intensify with HFpEF across the T2DM spectrum.

In recent years, LA function has been emphasized in the assessment of diastolic dysfunction and may represent the latent development of LV diastolic dysfunction. The LA plays a crucial role in modulating LV filling and overall cardiovascular performance [19]. LA strain is a more sensitive parameter for the diagnosis of HFpEF than LA volume [37, 40]. Our study demonstrated that patients with T2DM and HFpEF had reduced LA reservoir strain and increased LA booster strain compared to patients with T2DM without HFpEF. A previous study found that patients with HFpEF had reduced LA reservoir strain, LA conduit strain, and LA booster strain compared to controls [20]. The LA reservoir strain is affected by the descent of the LV basal segment during systole and the LV end-systolic volume. The LA conduit strain is reciprocally related to the reservoir function, but by necessity is closely related to LV relaxation and compliance. The LA booster strain depends on LV end-diastolic pressures and LV systolic reserve [19]. Increases in LA booster strain have been reported in HCM but not in patients with T2DM. [19, 20]. We hypothesized that the elevated LA booster strain in patients with T2DM, along with reductions in LA reservoir strain and LA conduit strain, may indicate a milder form of compensated diastolic dysfunction than the severe diastolic dysfunction observed in patients with HFpEF. It has been reported

Table 6 Receiver operating characteristic curve analysis for the detection of HFpEF

	AUC	95%CI	*P*-value	Cutoff value	Sensitivity	Specificity	PPV	NPV
Total population (n = 206)								
Global rest PI	0.735	0.656–0.813	< 0.0001	0.11*	0.73	0.80	0.67	0.84
Global stress PI	0.848	0.794–0.901	< 0.0001	0.16*	0.95	0.67	0.61	0.96
Global MPRI, ratio	0.808	0.749–0.867	< 0.0001	1.30*	0.93	0.72	0.65	0.95
Longitudinal PDSR, s^{-1}	0.591	0.509–0.672	0.0311	1.08*	0.72	0.53	0.46	0.77
Circumferential PDSR, s^{-1}	0.722	0.646–0.799	< 0.0001	0.78*	0.51	0.92	0.78	0.77
LA reservoir, %	0.752	0.683–0.822	< 0.0001	42.77*	0.76	0.80	0.67	0.85
LA conduit, %	0.595	0.511–0.678	0.0245	30.94*	0.91	0.36	0.44	0.87
LA booster, %	0.857	0.804–0.910	< 0.0001	16.70*	0.91	0.79	0.71	0.94
T2DM population (n = 156)								
Mean E/e', ratio	0.897	0.841–0.954	< 0.0001	15	0.76	0.94	0.91	0.83
LAVI, mL/m^2	0.690	0.609–0.773	< 0.0001	34	0.46	0.90	0.79	0.67
Global rest PI	0.740	0.650–0.831	< 0.0001	0.11*	0.73	0.85	0.80	0.80
Global stress PI	0.803	0.732–0.874	< 0.0001	0.14*	0.70	0.88	0.82	0.78
Global MPRI, ratio	0.740	0.661–0.819	< 0.0001	1.30*	0.93	0.60	0.65	0.92
Radial PSSR, s^{-1}	0.651	0.555–0.747	0.0012	1.90*	0.97	0.59	0.66	0.97
Circumferential PDSR, s^{-1}	0.700	0.616–0.784	< 0.0001	0.78*	0.51	0.90	0.81	0.70
LA reservoir, %	0.679	0.590–0.768	< 0.0001	42.77*	0.76	0.71	0.68	0.78
LA booster, %	0.790	0.717–0.864	< 0.0001	16.70*	0.91	0.68	0.70	0.90

PI perfusion index, *MPRI* myocardial perfusion reserve index, *PDSR* peak diastolic strain rate, *LA* left atrial, E/e', early filling velocity on transmitral Doppler/early relaxation velocity on tissue Doppler, *LAVI* left atrial volume index, *PSSR* peak systolic strain rate;

*Optimal cutoff value

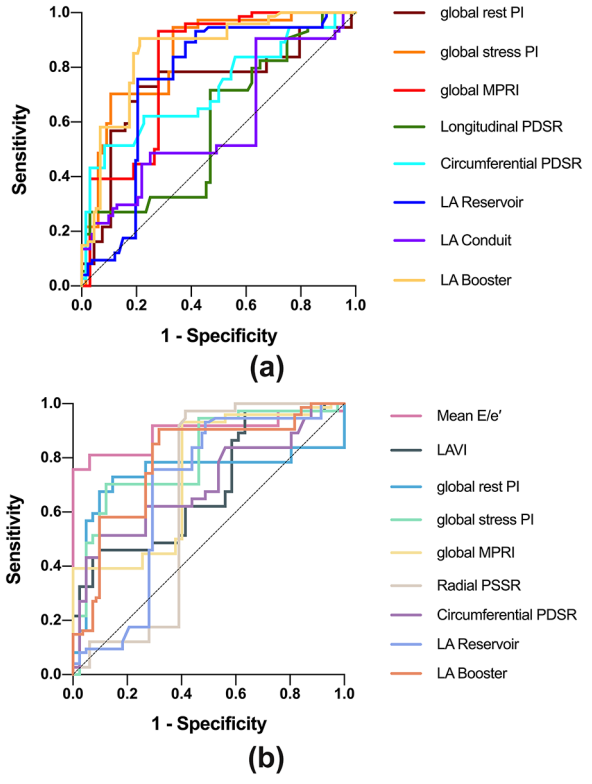

Fig. 4 ROC analyses for detecting HFpEF in all participants (**a**) and T2DM patients (**b**). Global stress PI, global MPRI, and LA Booster provided the highest AUC alone among all participants. Apart from echocardiographic parameters, global rest PI, global stress PI, global MPRI, and LA Booster provided the highest AUC alone in T2DM patients

that there is an initial increase in LA booster strain during the early stages of impaired LV relaxation, followed by a progressive decompensation of global LA performance as diastolic dysfunction worsens in the later stages of the disease [41] and these findings are in line with our hypothesis.

The reductions in global rest PI, global stress PI, and global MPRI suggest that myocardial perfusion impairment develops and worsens in patients with T2DM as the disease progresses, and this is consistent with prior research [23, 24, 38]. Global MPRI reduced gradually in patients with T2DM from the non-HFpEF stage to the HFpEF stage, indicating coronary microvascular response to adenosine stress is severely compromised. It is noteworthy that the association between diastolic dysfunction and myocardial perfusion in patients with T2DM remains largely unexplored and this should not be ignored. The association between impaired myocardial perfusion reserve and diastolic dysfunction in patients with T2DM has been identified by using echocardiography and myocardial perfusion scintigraphy [42]. Liu et al. found that LV longitudinal PDSR was significantly associated with the upslope and time to maximum signal intensity, suggesting a possible mechanistic link between impaired myocardial perfusion and subclinical myocardial dysfunction in patients with T2DM [38]. Our study found that LV longitudinal PDSR, LV circumferential PDSR, LA reservoir strain, and LA conduit strain were positively associated with global MPRI. Furthermore, multivariate linear regression analysis demonstrated

that LA reservoir strain was independently associated with global MPRI, whereas LA booster strain was independently associated with global rest PI, global MPRI, and HbA1c levels. The results of our study support the hypothesis that impaired myocardial perfusion contributes to myocardial dysfunction in patients with T2DM. Further research is needed to elucidate the underlying mechanisms while interventional trials aimed at reversing myocardial perfusion defects in patients with T2DM are warranted to improve myocardial function and prognosis.

We also explored the interdependence of myocardial perfusion and myocardial dysfunction that has never been studied before. Abnormal myocardial perfusion in patients with T2DM contributes to cardiac strain and functional changes, as verified by several studies [43, 44]. Our study found that the difference in LA reservoir strain and LA booster strain between patients with T2DM with and without HFpEF was totally mediated by global MPRI that suggests myocardial microcirculation may be associated with myocardial function, emphasizing the essential role of efficient energy production in normal myocardial contraction [45]. Based on our findings, we speculate that the effect of microcirculation on myocardial deformation may be explained by a disorder in the myocardial microcirculation, myocardial interstitium, and myocardial cells that harms nutrient and oxygen delivery and energy production, compromises myocardial contractility and relaxation, and eventually leads to myocardial dysfunction.

ROC analysis showed that LA booster, global stress PI and global MPRI had the accurate diagnostic efficacy in HFpEF. Previous study has demonstrated the limitations of conventional diagnostic tools and the emerging role of advanced imaging techniques such as LA strain, which is a more accurate way to measure heart function in patients with HFpEF [46]. While LAVI has traditionally been used to assess atrial size and pressure, our study found that it is inferior to myocardial perfusion and LA strain when diagnosing HFpEF in patients with T2DM, indicating that functional measures of the LA, such as strain, provide more relevant clinical information than mere volumetric assessments. Our findings suggest that incorporating LA strain and myocardial perfusion into the diagnostic procedure for HFpEF improves diagnostic accuracy significantly. Serial assessments of myocardial perfusion and LA strain can help monitor disease progression and the efficacy of therapeutic therapies, providing a dynamic assessment of patient status.

Limitations

Despite these meaningful results, our study has several limitations. First, the cross-sectional design prevented us from commenting on the timing of the events and determining a causal relationship or any direction of causality. Second, there may be potential selection bias in our study. Third, as this was a single-center study, our findings require validation through multicenter studies.

Conclusions

Patients with T2DM and HFpEF, but without CAD, exhibited significant diastolic dysfunction, a further reduction in LA reservoir function, and more severe impairment of myocardial perfusion, along with increased LA booster function that is a compensatory response in HFpEF. Myocardial perfusion and LA strain may prove valuable for diagnosing and managing HFpEF in the future. Our study is the first to evaluate of the damage and intricate interactions between myocardial strain and perfusion in patients with T2DM and HFpEF. We speculate that an abnormal and deteriorative diabetic metabolism may mediate a reduction in LA reservoir function and elevation in LA booster function by impairing global MPRI in patients with T2DM and HFpEF, suggesting a possible mechanistic link between microcirculation impairment and cardiac dysfunction in diabetes.

Abbreviations

T2DM	Type 2 diabetes mellitus
CMR	Cardiovascular magnetic resonance
HFpEF	Heart failure with preserved ejection fraction
LV	Left ventricular
LA	Left atrial
PSSR	Peak systolic strain rate
PDSR	Peak diastolic strain rate
PI	Perfusion index
MPRI	Myocardial perfusion reserve index
AUC	Area under curve
DM	Diabetes mellitus
CAD	Coronary artery disease
CMD	Microvascular dysfunction
CVD	Cardiovascular disease
HF	Heart failure
HCM	Hypertensive cardiomyopathy
ESC	European Society of Cardiology
LVEF	Left ventricular ejection fraction
NP	Natriuretic peptide
eGFR	Estimated glomerular filtration rate
RWT	Relative wall thickness
LVMI	Left ventricular mass index
LAVI	Left atrial volume index
BSA	Body surface area
E	Peak velocity in early diastole of mitral valve inflow
e′	Early diastolic velocity of the mitral valve annulus
E/e′	Early filling velocity on transmitral Doppler/early relaxation velocity on tissue Doppler
eGFR	Estimated glomerular filtration rate
HbA1c	Glycosylated hemoglobin
ECG	Electrocardiographic
bSSFP	Balanced steady-state free precession
TR	Repetition time
TE	Echo time
IR-EPI	Inversion recovery echo-planar imaging
LGE	Late gadolinium enhancement
PSIR	Segmented-turbo-FLASH–phase-sensitive inversion recovery
ROI	Region of interest
ICC	Intraclass correlation coefficient
SD	Standard deviation
RO	Receiver operating characteristic
PPV	Positive predictive value

NPV	Negative predictive value
Fib-4	Fibrosis-4 index
BNP	B-type natriuretic peptide
pro-BNP	Pro-B-type natriuretic peptide
UA	Uric acid
TC	Total cholesterol
BMI	Body mass index
Scr	Serum creatinine
IQR	Interquartile range
HR	Heart rate
TyG-BMI	Triglyceride glucose-body mass index
FBG	Fasting blood glucose
TG	Total triglyceride
HDL	High-density lipoprotein
LDL	Low-density lipoprotein

Supplementary Information

The online version contains supplementary material available at https://doi.org/10.1186/s12933-024-02380-2.

Supplementary Material 1.

Acknowledgements
Not applicable.

Author contribution
XNL participated in the study design, performed the statistical analysis, and drafted the manuscript. CXS and JWP contributed to the study design and contributed to the preparation, quality control of data and algorithms, editing, and review of the manuscript. YTL and KS participated in data acquisition and contributed to data analysis and interpretation. WKM contributed to the preparation of the manuscript. HYX and DZQY assisted with the data collection. All authors read and approved the final manuscript.

Funding
This work was supported by the Medical Innovation Research Project of Shanghai 2021 "Science and Technology Innovation Action Plan" (21Y11909400) and the Pioneer Program of Shanghai 2023 "Science and Technology Plan Project" (23TS1400700).

Data availability
The datasets used and analyzed during the current study are available from the corresponding author upon reasonable request.

Declarations

Ethics approval and consent to participate
The study complied with the Declaration of Helsinki and was approved by the Institutional Ethics Committee of Shanghai Sixth People's Hospital Affiliated to Shanghai Jiao Tong University School of Medicine, Shanghai Jiao Tong University (Shanghai, China). Written informed consents were obtained from all the study participants.

Consent for publication
Not applicable.

Competing interests
The authors declare no competing interests.

Author details
[1]Department of Cardiology, Shanghai Sixth People's Hospital Affiliated to Shanghai Jiao Tong University School of Medicine, Shanghai 200233, China

Received: 6 April 2024 / Accepted: 29 July 2024
Published online: 16 August 2024

References

1. American Diabetes Association Professional Practice Committee, ElSayed NA, Aleppo G, Bannuru RR, Bruemmer D, Collins BS, et al. 2. Diagnosis and classification of diabetes: *standards of Care in Diabetes—2024*. Diabetes Care. 2024;47:S20–42.
2. Patel MR, Peterson ED, Dai D, Brennan JM, Redberg RF, Anderson HV, et al. Low diagnostic yield of Elective Coronary Angiography. N Engl J Med. 2010;362:886–95.
3. Ong P, Camici PG, Beltrame JF, Crea F, Shimokawa H, Sechtem U, et al. International standardization of diagnostic criteria for microvascular angina. Int J Cardiol. 2018;250:16–20.
4. Sara JD, Taher R, Kolluri N, Vella A, Lerman LO, Lerman A. Coronary microvascular dysfunction is associated with poor glycemic control amongst female diabetics with chest pain and non-obstructive coronary artery disease. Cardiovasc Diabetol. 2019;18:22.
5. Marx N, Federici M, Schütt K, Müller-Wieland D, Ajjan RA, Antunes MJ, et al. 2023 ESC guidelines for the management of cardiovascular disease in patients with diabetes. Eur Heart J. 2023;44:4043–140.
6. Cavender MA, Steg PG, Smith SC, Eagle K, Ohman EM, Goto S, et al. Impact of diabetes Mellitus on hospitalization for heart failure, Cardiovascular events, and death: outcomes at 4 years from the Reduction of Atherothrombosis for Continued Health (REACH) Registry. Circulation. 2015;132:923–31.
7. McAllister DA, Read SH, Kerssens J, Livingstone S, McGurnaghan S, Jhund P, et al. Incidence of hospitalization for heart failure and case-fatality among 3.25 million people with and without diabetes Mellitus. Circulation. 2018;138:2774–86.
8. Maceira AM, Guardiola S, Ripoll C, Cosin-Sales J, Belloch V, Salazar J. Detection of subclinical myocardial dysfunction in cocaine addicts with feature tracking cardiovascular magnetic resonance. J Cardiovasc Magn Reson. 2020;22:70.
9. Schuster A, Hor KN, Kowallick JT, Beerbaum P, Kutty S. Cardiovascular magnetic resonance myocardial feature tracking: concepts and clinical applications. Circ Cardiovasc Imaging. 2016;9:e004077.
10. Muser D, Castro SA, Santangeli P, Nucifora G. Clinical applications of feature-tracking cardiac magnetic resonance imaging. World J Cardiol. 2018;10:210–21.
11. Shenoy C, Romano S, Hughes A, Okasha O, Nijjar PS, Velangi P, et al. Cardiac magnetic resonance feature tracking global longitudinal strain and prognosis after heart transplantation. JACC Cardiovasc Imaging. 2020;13:1934–42.
12. Von Bibra H, St John Sutton M. Diastolic dysfunction in diabetes and the metabolic syndrome: promising potential for diagnosis and prognosis. Diabetologia. 2010;53:1033–45.
13. Stratmann B, Tschoepe D. Heart in diabetes: not only a Macrovascular Disease. Diabetes Care. 2011;34:S138–44.
14. Gupta S, Matulevicius SA, Ayers CR, Berry JD, Patel PC, Markham DW, et al. Left atrial structure and function and clinical outcomes in the general population. Eur Heart J. 2013;34:278–85.
15. Hoit BD. Assessment of Left Atrial function by Echocardiography: Novel insights. Curr Cardiol Rep. 2018;20:96.
16. Santos ABS, Kraigher-Krainer E, Gupta DK, Claggett B, Zile MR, Pieske B, et al. Impaired left atrial function in heart failure with preserved ejection fraction. Eur J Heart Fail. 2014;16:1096–103.
17. Tsang TSM, Abhayaratna WP, Barnes ME, Miyasaka Y, Gersh BJ, Bailey KR, et al. Prediction of Cardiovascular outcomes with left atrial size. J Am Coll Cardiol. 2006;47:1018–23.
18. Thomas L, Marwick TH, Popescu BA, Donal E, Badano LP. Left atrial structure and function, and left ventricular diastolic dysfunction. J Am Coll Cardiol. 2019;73:1961–77.
19. Hoit BD. Left atrial size and function. J Am Coll Cardiol. 2014;63:493–505.
20. Kowallick JT, Kutty S, Edelmann F, Chiribiri A, Villa A, Steinmetz M, et al. Quantification of left atrial strain and strain rate using Cardiovascular magnetic resonance myocardial feature tracking: a feasibility study. J Cardiovasc Magn Reson. 2014;16:60.
21. Raafs AG, Vos JL, Henkens MTHM, Slurink BO, Verdonschot JAJ, Bossers D, et al. Left atrial strain has Superior Prognostic Value to ventricular function and delayed-enhancement in dilated cardiomyopathy. JACC Cardiovasc Imaging. 2022;15:1015–26.
22. Zhou H, An D-A, Ni Z, Xu J, Zhou Y, Fang W, et al. Incremental diagnostic value of CMR-derived LA strain and strain rate in dialysis patients with HFpEF. Eur J Radiol. 2022;151:110285.
23. Sørensen MH, Bojer AS, Pontoppidan JRN, Broadbent DA, Plein S, Madsen PL, et al. Reduced myocardial Perfusion Reserve in Type 2 diabetes is caused by

increased perfusion at Rest and decreased maximal perfusion during stress. Diabetes Care. 2020;43:1285–92.
24. Sørensen MH, Bojer AS, Broadbent DA, Plein S, Madsen PL, Gæde P. Cardiac perfusion, structure, and function in type 2 diabetes mellitus with and without diabetic complications. Eur Heart J - Cardiovasc Imaging. 2020;21:887–95.
25. Scatteia A, Baritussio A, Bucciarelli-Ducci C. Strain imaging using cardiac magnetic resonance. Heart Fail Rev. 2017;22:465–76.
26. Chamsi-Pasha MA, Zhan Y, Debs D, Shah DJ. CMR in the evaluation of diastolic dysfunction and phenotyping of HFpEF. JACC Cardiovasc Imaging. 2020;13:283–96.
27. McDonagh TA, Metra M, Adamo M, Gardner RS, Baumbach A, Böhm M, et al. 2021 ESC guidelines for the diagnosis and treatment of acute and chronic heart failure. Eur Heart J. 2021;42:3599–726.
28. Kramer CM, Barkhausen J, Bucciarelli-Ducci C, Flamm SD, Kim RJ, Nagel E. Standardized cardiovascular magnetic resonance imaging (CMR) protocols: 2020 update. J Cardiovasc Magn Reson. 2020;22:17.
29. Nagel E, Klein C, Paetsch I, Hettwer S, Schnackenburg B, Wegscheider K, et al. Magnetic resonance perfusion measurements for the Noninvasive detection of coronary artery disease. Circulation. 2003;108:432–7.
30. Bansal M, Leano RL, Marwick TH. Clinical Assessment of Left Ventricular Systolic Torsion: effects of myocardial infarction and ischemia. J Am Soc Echocardiogr. 2008;21:887–94.
31. Rüssel IK, Götte MJW, Bronzwaer JG, Knaapen P, Paulus WJ, Van Rossum AC. Left ventricular torsion. JACC Cardiovasc Imaging. 2009;2:648–55.
32. Lin J-L, Sung K-T, Su C-H, Chou T-H, Lo C-I, Tsai J-P, et al. Cardiac structural remodeling, longitudinal systolic strain, and Torsional mechanics in lean and nonlean dysglycemic Chinese adults. Circ Cardiovasc Imaging. 2018;11:e007047.
33. Kishi S, Gidding SS, Reis JP, Colangelo LA, Venkatesh BA, Armstrong AC, et al. Association of Insulin Resistance and glycemic metabolic abnormalities with LV structure and function in Middle Age. JACC Cardiovasc Imaging. 2017;10:105–14.
34. Rademakers FE, Rogers WJ, Guier WH, Hutchins GM, Siu CO, Weisfeldt ML, et al. Relation of regional cross-fiber shortening to wall thickening in the intact heart. Three-dimensional strain analysis by NMR tagging. Circulation. 1994;89:1174–82.
35. Van Dalen BM, Tzikas A, Soliman OII, Heuvelman HJ, Vletter WB, Ten Cate FJ, et al. Assessment of Subendocardial contractile function in aortic stenosis: a study using Speckle Tracking Echocardiography. Echocardiography. 2013;30:293–300.
36. Van Dalen BM, Tzikas A, Soliman OII, Kauer F, Heuvelman HJ, Vletter WB, et al. Left ventricular twist and untwist in aortic stenosis. Int J Cardiol. 2011;148:319–24.
37. Liu J-H, Wu M-Z, Li S-M, Chen Y, Ren Q-W, Lin Q-S, et al. Association of serum uric acid with biventricular myocardial dysfunction in patients with type 2 diabetes mellitus. Nutr Metab Cardiovasc Dis. 2021;31:2912–20.
38. Liu X, Yang Z, Gao Y, Xie L, Jiang L, Hu B, et al. Left ventricular subclinical myocardial dysfunction in uncomplicated type 2 diabetes mellitus is associated with impaired myocardial perfusion: a contrast-enhanced cardiovascular magnetic resonance study. Cardiovasc Diabetol. 2018;17:139.
39. Shen L-T, Jiang L, Zhu Y-W, Shen M-T, Huang S, Shi R, et al. Additive effect of aortic regurgitation degree on left ventricular strain in patients with type 2 diabetes mellitus evaluated via cardiac magnetic resonance tissue tracking. Cardiovasc Diabetol. 2022;21:37.
40. Telles F, Nanayakkara S, Evans S, Patel HC, Mariani JA, Vizi D, et al. Impaired left atrial strain predicts abnormal exercise haemodynamics in heart failure with preserved ejection fraction. Eur J Heart Fail. 2019;21:495–505.
41. Murata M, Iwanaga S, Tamura Y, Kondo M, Kouyama K, Murata M, et al. A real-time three-dimensional echocardiographic quantitative analysis of left atrial function in Left Ventricular Diastolic Dysfunction. Am J Cardiol. 2008;102:1097–102.
42. Poulsen MK, Henriksen JE, Dahl J, Johansen A, Gerke O, Vach W, et al. Left ventricular diastolic function in type 2 diabetes Mellitus: Prevalence and Association with myocardial and vascular disease. Circ Cardiovasc Imaging. 2010;3:24–31.
43. From AM, Scott CG, Chen HH. Changes in Diastolic Dysfunction in Diabetes Mellitus over Time. Am J Cardiol. 2009;103:1463–6.
44. Larghat AM, Swoboda PP, Biglands JD, Kearney MT, Greenwood JP, Plein S. The microvascular effects of insulin resistance and diabetes on cardiac structure, function, and perfusion: a cardiovascular magnetic resonance study. Eur Heart J - Cardiovasc Imaging. 2014;15:1368–76.
45. Miki T, Yuda S, Kouzu H, Miura T. Diabetic cardiomyopathy: pathophysiology and clinical features. Heart Fail Rev. 2013;18:149–66.
46. Reddy YNV, Borlaug BA. Heart failure with preserved ejection fraction. Curr Probl Cardiol. 2016;41:145–88.

Publisher's Note